

## P1.5 DETAILED SURFACE OBSERVATIONS DURING THE LAHOMA HAIL AND WINDSTORM

Dale A. Morris and Mark A. Shafer

Oklahoma Climatological Survey, University of Oklahoma,  
Norman, Oklahoma

### 1. INTRODUCTION

On August 17, 1994, extreme wind and hail damage occurred in north-central Oklahoma from a weakening, complex of thunderstorms that moved from southern Kansas into a thermodynamically favorable environment in western Oklahoma. The Oklahoma Mesonet (Mesonet; Brock *et al.* 1995) is an automated environmental monitoring network with at least one station in each of Oklahoma's 77 counties. By early afternoon on 17 August, it measured surface temperatures between 35° C and 40° C and surface dew points between 18° C and 21° C in western Oklahoma ahead of the storm complex (Morris and Janish 1996; see their Fig. 1). This rich environment allowed the storm to reintensify to extraordinary limits as it passed directly over the Mesonet site located 1 mile west-southwest of Lahoma in Garfield County.

At the Lahoma site, the propeller-vane wind monitor at 10 m above the surface recorded *sustained* wind speeds of 34.6 m/s between 1945 and 1950 UTC, and peak gusts exceeding 50 m/s between 1945 and 1950 and again between 1950 and 1955 (see Fig. 3). In addition, a cup anemometer at 2 m measured sustained winds over 25 m/s between 1945 and 1955 before wind-driven golfball to tennis ball sized hail destroyed the wind instruments. Eyewitnesses described some of the hail as chunks of ice measuring 10 cm by 15 cm, and reported hail depths of up to 15 cm. A Mesonet technician who visited the Lahoma site after the storm described the landscape as being "very winterlike because the hail stripped every leaf off the trees in a 5 mile area." Most structures had paint stripped off the north and east sides of the buildings and many had broken windows. Two people were treated for hypothermia after hail smashed the windows and accumulated inside their car. Other witnesses compared the approaching storm to the Dust Bowl of the 1930's as they saw a large, dark cloud approaching from the north (Les Lemon, personal communication).

The original design of the Oklahoma Mesonet (Elliott *et al.* 1992) called for telecommunicating three sets of five-minute observations every fifteen minutes from the remote sites to the base station in Norman. However, to monitor an annular solar eclipse that passed over Oklahoma on 10 May 1994, modifications were made to the remote datalogger programs to allow *one-minute* observations to be recorded and transmitted. (McPherson 1995). Because of the data storage in the dataloggers, and because of the two-way nature of the radio communications via the Oklahoma Law Enforcement Telecommunications System (OLETS; Crawford and Long 1993), the capability exists to retrieve one-minute observations from a Mesonet site up to six hours after an event. Mesonet staff exercised this capability after the Lahoma storm and retrieved one-minute readings of air temperature at 1.5 m above the surface (TAIR), solar radiation (SRAD), pressure (PRES), and wind speed (WSPD) and direction (WDIR) at 10 m from several sites in north central Oklahoma (Fig. 1). Due to a power outage at the Kingfisher County Sheriff's

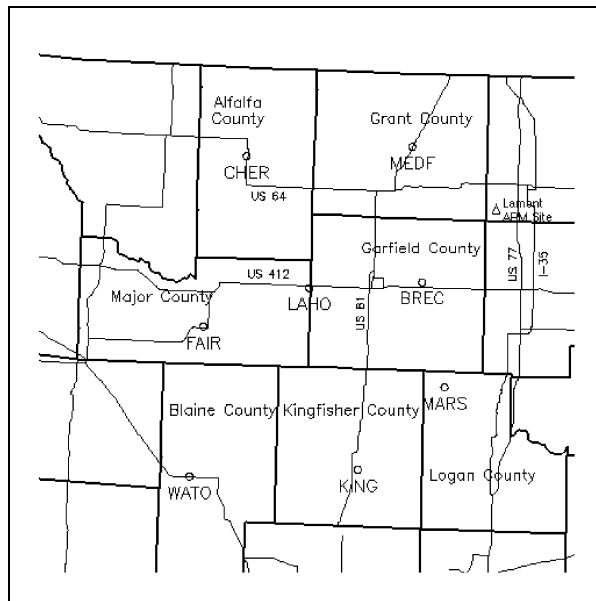


**Figure 1.** Locations of the Mesonet sites used in this study. Every site except KING reported one-minute data. Federal highways are included for geographic reference. The Lamont ARM site is also indicated.

*Corresponding author address:* Dale A. Morris,  
Oklahoma Climatological Survey, 100 E. Boyd, Suite  
1210, Norman, OK 73019; e-mail:  
dmorris@uoknor.edu.

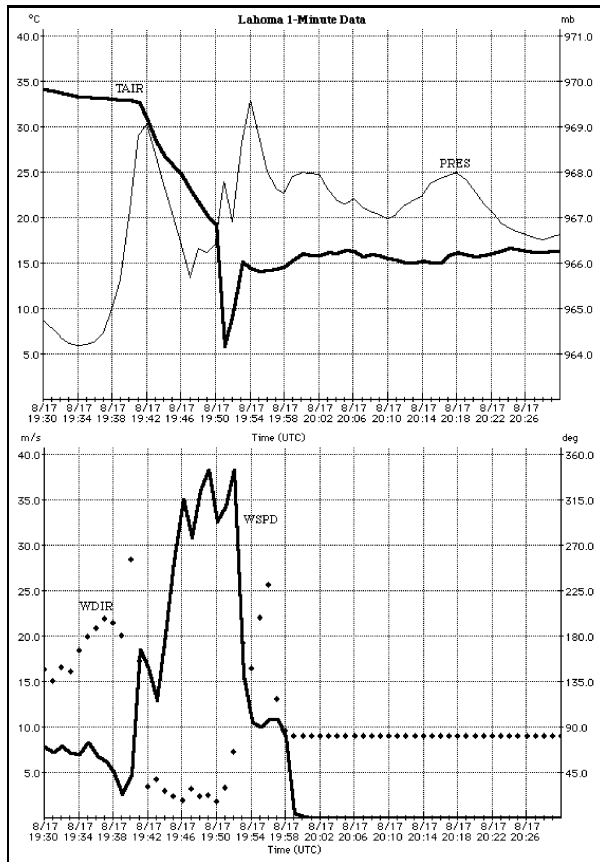


**Figure 2.** Time series plot of one-minute resolution data from the Lahoma Mesonet site. Top: air temperature at 1.5 m (TAIR; heavy line) in °C and station pressure (PRES; light line) in mb. Bottom: wind speed at 10 m (WSPD; heavy line) in m/s and wind direction at 10 m (WDIR; diamonds). The readings after 1954 occurred after the wind sensors were damaged.

Office, one-minute data from the KING site were unavailable; the five-minute observations were retrieved, however. This paper presents a summary and an analysis of this unique set of detailed surface observations.

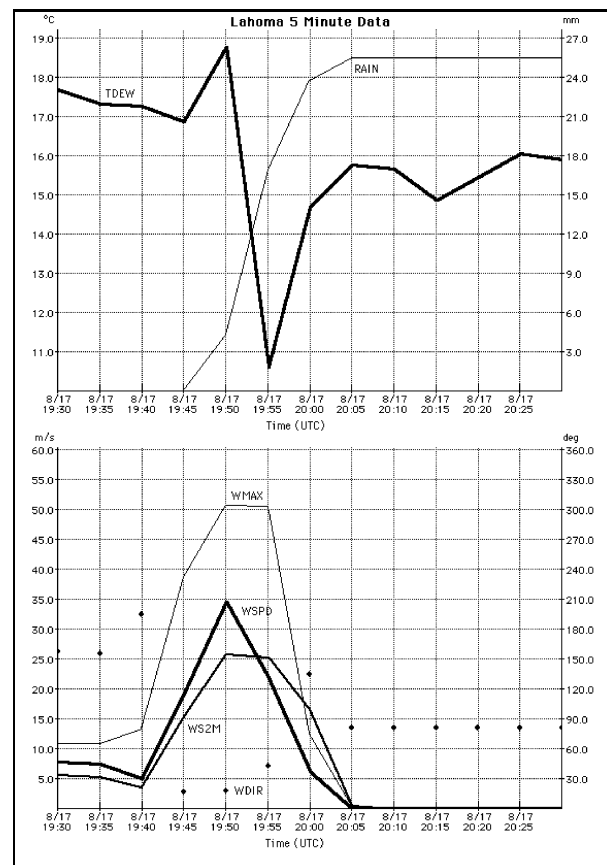
## 2. LAHOMA TIME SERIES

Figure 2 presents one-minute average readings of TAIR, PRES, WSPD, and WDIR at the Lahoma Mesonet site (LAHO) from 1930 through 2030 UTC. Five-minute

<sup>1</sup>Since the Lahoma event, the datalogger program has been modified to calculate one-minute averages of each parameter that is normally averaged over a five-minute period and to report these averages upon request. See Brock *et al.* (1995) for more information on sampling and averaging periods of Mesonet parameters.

averages of several parameters that were not included in the one-minute datalogger program<sup>1</sup> are displayed in Figure 3. From these data a timeline of events that occurred at and/or near the Lahoma site can be constructed.

Based upon the traces in Figure 2, the gust front from the Lahoma storm passed the LAHO site at approximately 1942 UTC. At this time, the pressure began to fall rapidly, the wind shifted to the northeast, and the temperature began to decrease. It should be noted that the datalogger incorrectly reported several of the one-minute average wind directions when the samples included directions from both west of north and east of north. The five-minute averages in Figure 3, however, were correctly calculated. Additional evidence that supports the gust frontal passage at 1942 includes the facts that rain began to fall between 1945 and 1950 (Fig. 3) and that a decrease of 9° C in 9-m air temperature



**Figure 3.** Time series plot of five-minute resolution data from the Lahoma Mesonet site. Top: dew point (TDEW; heavy line) in °C and accumulated rainfall (RAIN; light line) in mm. Bottom: peak gust at 10 m (WMAX; lightest line), average wind speed at 2 m (WS2M; medium line), average wind speed at 10 m (WSPD; heavy line), and wind direction at 10 m (diamonds). All wind speeds are in m/s.

occurred between 1940 and 1945 (not shown).

Lemon and Parker (1996) documented a series of mesocyclones occurring in the Lahoma storm from an analysis of Level II WSR-88D data from the Twin Lakes radar. They identified a mesocyclone first appearing southeast of Lahoma at 1944. This mesocyclone may be partially responsible for the pressure fall ending at 1947.

The large wind speed maxima at 1946, 1949, and 1952 likely resulted from an intense downburst that may have coincided with the onset of precipitation. The heaviest precipitation occurred between 1950 and 1955. Each of the three peaks in the one-minute average wind speeds were followed by the expected pressure rises. These three peaks may indicate that there were three separate downbursts, or that one downburst actually thrust three separate pulses of air toward the surface. At any rate, eyewitness reports and the damage swath indicate that the strong winds first came from the north and subsequently from an easterly direction -- facts that are corroborated by Mesonet observations. The direction associated with the third downburst or downburst pulse suggests that the downburst was located to the east or northeast of the LAHO site. The large hail that accompanied what may have been the final gust of wind rendered both the 10-m wind monitor and 2-m wind sentry useless. The large gust of wind also wrapped the cables connecting the wind monitor and the 9-m thermistor to the datalogger around the wind monitor.

One of the more puzzling aspects of the one-minute averages is the sudden temperature decrease to 5.9° C at 1952. Several hypotheses to explain this decrease have been investigated. The first hypothesis is that the cool temperatures were associated with the downburst. If this were the case, then a logical question to ask is from what altitude did the cold air descend. To answer this, two special soundings launched at nearby Lamont by the ARM (Atmospheric Radiation Measurement; Stokes and Schwartz 1994) program were examined. The equivalent potential temperature of the surface parcel was calculated, but no match could be found in either of two soundings (one prior to and one just after the Lahoma event). A portion of the 5.9° C reading may be attributed to the downburst, but it is unlikely that the downburst is the only mechanism responsible.

Another hypothesis is the "wetting effect" of cold water on a radiation shield. Since there was precipitation and large hail at the time of the 5.9° C reading, the radiation shield that enclosed the temperature and relative humidity (T&RH) sensor was drenched with water having a temperature near freezing. Our theory is that the 30 to 50 m/s wind aided the evaporation of the cold water thereby biasing the temperature inside the shield, making it cooler than ambient. The relative humidity (a five-minute average) during this time period ranged from 83% to 92%. An experiment was staged to test the feasibility

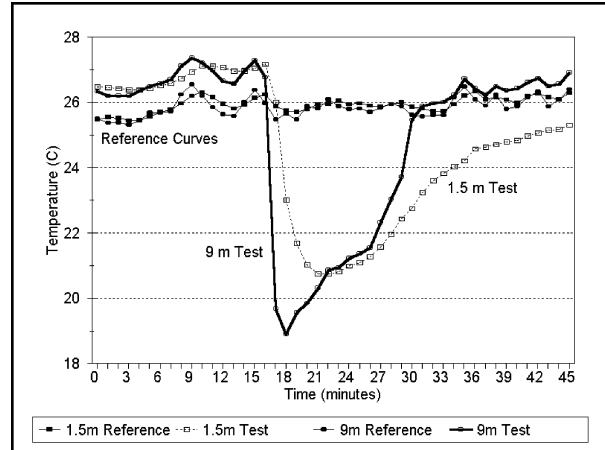


**Figure 4.** Results of cold-water test. The water was poured over the test radiation shield for 90 seconds beginning at minute 15. The 1.5 m T&RH sensor is larger than the 9 m sensor so it has a larger thermal mass and a slower response.

of this hypothesis. Two sets of sensors, like those used at 1.5 m and 9 m, were paired and housed in identical radiation shields. Ice water was poured over one of the shields for 90 seconds during warm (26° C) and relatively windy (10 m/s gusting to 14 m/s) but dry (30% relative humidity) conditions. Figure 4 shows the results from this simple experiment. It indicates that the 5.9° C Lahoma temperature reading probably did not result from this mechanism, because the 1.5 m sensor was incapable of responding quickly to a step function input of this magnitude. Additionally, the test was performed in conditions more favorable for evaporation (hence more cooling) than during the Lahoma event. Figure 4 also indicates that significant temperature error can result during precipitation if ambient conditions are favorable for evaporation.

The final theory is that the high winds at the LAHO site may have caused a temporary loose connection in the cabling of the T&RH sensor. When the datalogger receives no input voltage from a thermistor, it assumes the temperature to be -273.1° C. Even though the technician who inspected the site the following day found no problems with the T&RH sensor, one 3-second sample of -273.1° C could transform a one-minute average reading of 20° C to about 5° C. Thus, a loose connection is likely responsible not only for the 5.9° C temperature, but also for the 5-minute average 10° C dewpoint at 1955 (Fig. 3) because the 5-minute average temperature from 1950 to 1955 was reported as 11.9° C. This point underscores the importance and difficulty of quality assurance routines for automated networks (Shafer and Hughes 1996) and the repercussions of blindly accepting a report from any meteorological instrument.

### 3. OBJECTIVE ANALYSIS

In order to place the events that occurred at the LAHO site into context with conditions at neighboring sites, an objective analysis of the one-minute data was performed. Since one-minute observations from the KING site were unavailable, its five-minute observations were interpolated to one-minute intervals. A two-pass Barnes (1973)

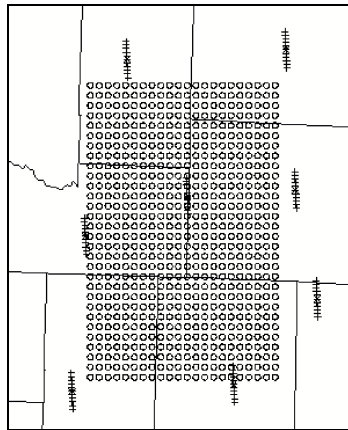


**Figure 5.** Analysis grid for objective analysis. Hash marks indicate results of time-to-space conversion.

analysis utilizing a time-to-space conversion technique was performed on a grid having a 3 km mesh (Fig. 5). The time-to-space conversion used a time window of  $\pm 5$  minutes. The translation velocity of 19.5 m/s from 341° was determined subjectively using NIDS (NEXRAD Information Dissemination Service) images from the Twin Lakes (KTLX) and Vance AFB (KVNK) radars.

The Barnes technique with time-to-space conversion is not necessarily well-suited for a *quantitative* analysis of this particular situation. In this case, a quasi-steady state assumption is not valid. Moreover, the observations are clustered spatially. Barnes (1994) showed that the scheme has better sampling properties when stations are *uniformly arrayed*. Nevertheless, the technique is useful for *qualitative* visualization.

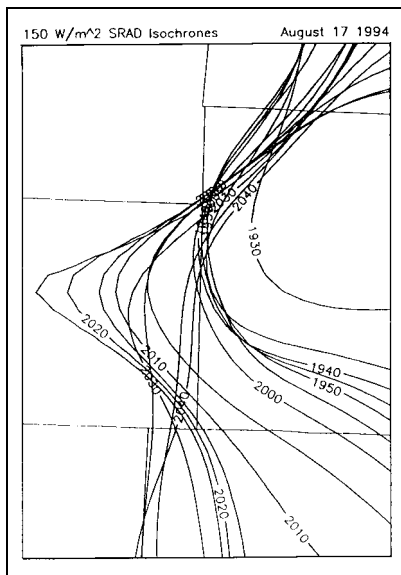


**Figure 6.** Five-minute isochrones of the  $150 \text{ W/m}^2$  SRAD isopleth.

An isochrone analysis of the  $150 \text{ W/m}^2$  SRAD isopleth is presented in Figure 6. The isochrones indicate that the cloud shield and dust associated with the Lahoma storm pushed westward until 2025 UTC when

it began to move toward the southeast. During this time, the storm itself moved southeastward. The early westward motion of the SRAD isopleths is supported by the eyewitness reports and by the motion of the outflow boundary that appeared on the KVNK imagery.

The pressure, temperature, and wind analyses are given in Figures 7a-7f. Pre-storm conditions are represented by the relatively low pressures over LAHO,

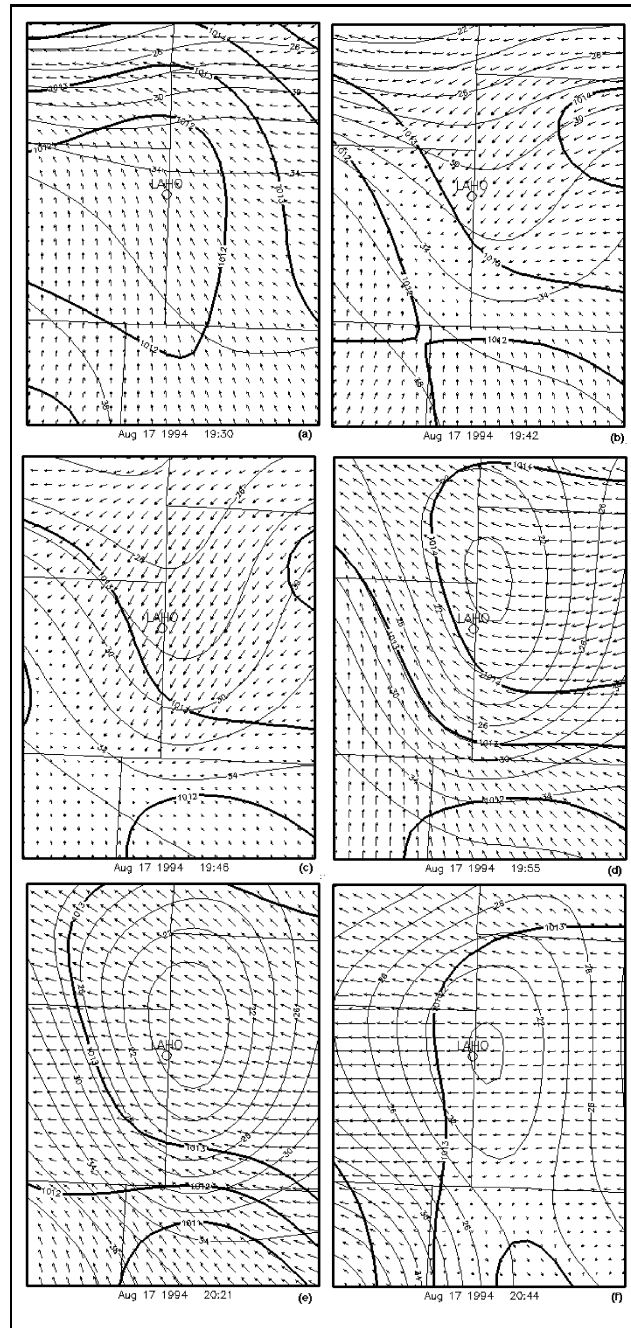


**Figure 7.** Isobars (heavy lines; 1 mb interval), isotherms (light lines; 2° C interval) and wind vectors for (a) 1930, (b) 1942, (c) 1946, (d) 1955, (e) 2021, and (f) 2044 UTC.

a weak temperature gradient in the southern two-thirds of the domain, and predominately southerly flow at 1930 UTC (Fig. 7a). By 1942 (Fig. 7b), the time of the passage of the gust front at the LAHO site, a mesohigh can be detected in the northeast portion of the domain, and cooler temperatures and a predominate northeasterly flow are apparent in the northern half of the grid. At the time of the first downburst (1946; Fig. 7c), stronger winds are located in the central portion of the grid, the temperatures have continued to decrease, but the pressure pattern remains similar to that observed four minutes earlier. At 1955 (Fig. 7d), the time of the third downburst pulse, the winds have a predominate easterly component in Garfield, western Alfalfa, and western Major counties. Surface pressures continue to increase due to the downburst which causes strengthening of the mesohigh. The spatial patterns shown in Figure 7d remain relatively constant, but varying in magnitude, until 2021 when pressures begin to fall in Kingfisher County as the storm approaches Kingfisher (Fig. 7e). Animated loops of the analysis indicate that the interpolation of Kingfisher five-minute resolution data to one-minute intervals seems artificially to slow the storm's southward motion. The spatial patterns likely changed before 2021, but without the KING one-minute data, it is impossible to gauge when this occurs. Figure 7f reveals that the storm created a mesohigh which extended south to Kingfisher and produced easterly flow throughout the domain. This easterly flow regime agrees with the composite wind field averaged over the storm's history as produced by Morris and Janish (1996). Figure 7f also shows that the area around Lahoma had a residual effect of lingering cool temperatures. The time-series plot of the LAHO temperatures (Fig. 2) indicates that temperatures remained slightly above 15° C while other locations (e.g., Kingfisher and El Reno) affected by the same storm (also with hail) had residual temperatures at least 5 to 10° C warmer than the Lahoma temperatures. While it cannot be proven with certainty, the latter locations likely were not influenced by a downburst and the cool temperatures it may have caused.

#### 4. SUMMARY

One-minute observations recorded by the Oklahoma Mesonet during the Lahoma hail and wind storm have been presented. The increased resolution of the data, compared to the five-minute averages normally obtained from the Mesonet, allowed the authors to conclude at least three separate downbursts occurred near the Lahoma site, each separated by a few minutes. The downbursts caused abnormally high pressure readings, and cool temperatures that lingered after the storm, than observed at other nearby locations. The Mesonet

observations presented in this paper also are consistent with eyewitness reports of the storm.

#### 5. ACKNOWLEDGEMENTS

The authors would like to dedicate this paper to the memory of David Shellberg, who was instrumental in collecting the one-minute data. Bill Wyatt provided information about the Lahoma Mesonet site, Fred Brock and Sherman Frederickson provided stimulating conversation about the instrumentation, and Ken Crawford provided helpful comments. Finally, David Grimsley and Jerry Brotzge assisted with the radiation shield experiment.

#### 6. REFERENCES

- Barnes, S.L., 1973: Mesoscale objective map analysis using weighted time-series observations. *NOAA Tech. Memo. ERL NSSL-62*, National Severe Storms Laboratory, Norman, OK, 60pp.
- \_\_\_\_\_, 1994: Applications of the Barnes objective analysis scheme. **11P** Effects of undersampling, wave position, and randomness. *J. Atmos. Ocean. Tech.*, **11**, 1433-1448.
- Brock, F.V., K.C. Crawford, R.L. Elliott, G.W. Cuperus, S.J. Stadler, H.L. Johnson, and M.D. Eilts, 1995: The Oklahoma Mesonet: A technical overview. *J. Atmos. Ocean. Tech.*, **12**, 5-19.
- Crawford, K.C., and B. Long, 1993: The design of a digital data communications system for the Oklahoma Mesonet. *9th Intl. Conf. on Interactive Info. and Proc. Systems*, Amer. Meteor. Soc. (not included in preprint volume but available from the author)
- Elliott, R.L., F.V. Brock, M.L. Stone, and S.L. Harp, 1992: Configuring the Oklahoma Mesonet of automated weather stations. Paper No. 922149, Intl. Summer Meeting; Amer. Soc. of Agricultural Engineers, Charlotte, NC.
- Lemon, L.R. and S. Parker 1996: The Lahoma storm deep convergence zone: its characteristics and role in storm dynamics and severity. *18th Conf. on Severe Local Storms*, Amer. Meteor. Soc.
- McPherson, R.A., 1995: Oklahoma schools view the 10 May 1994 eclipse. *Preprints, 4th Conf. on Education*, Amer. Meteor. Soc., 105-110.
- Morris, D.A., and P.R. Janish, 1996: The utility of mesoscale versus synoptic scale surface observations during the Lahoma hail and windstorm of 17 August 1994. *18th Conf. on Severe Local Storms*, Amer. Meteor. Soc.
- Shafer, M.A., and T.W. Hughes, 1996: Automated quality assurance of data from the Oklahoma Mesonet. *Preprints, 12th Intl. Conf. on Inter. Info. and Proc. Systems*, Amer. Meteor. Soc.
- Stokes, G.M., and S.E. Schwartz, 1994: The Atmospheric Radiation Measurement (ARM) Program: Programmatic background and design of the Cloud and Radiation Test Bed. *Bull. Amer. Meteor. Soc.*, **75**, 1201-1221.